Navigation Parameters Correction Technique Using Multiple View Geometry Methods

Victoria A. Sablina
Department of Electronic Computers
RSREU
Gagarina, 59/1
390005, Ryazan, Russia
sablina.v.a@evm.rsreu.ru

Anatoly I. Novikov
Department of Higher Mathematics
RSREU
Gagarina, 59/1
390005, Ryazan, Russia
novikovanatoly@yandex.ru

Michael B. Nikiforov
Department of Electronic Computers
RSREU
Gagarina, 59/1
390005, Ryazan, Russia
nikiforov.m.b@evm.rsreu.ru

Alexander A. Loginov
Department of Electronic Computers
RSREU
Gagarina, 59/1
390005, Ryazan, Russia
loginal@mail.ru

ABSTRACT

The problem of determining precisely the navigation parameters of an aircraft arise when constructing a multispectral computer vision system. In particular, these parameters are used to solve the image superimposition task. It is necessary to superimpose the aerial photograph registered from the on-board sensors and the image generated from the digital terrain map. Such superimposition will be successful only if this image is synthetized for the viewpoint based on the correct navigation parameters. However, the navigation parameters obtained from satellite and inertial navigation systems have inadmissible errors for this task. Thus it is required to reduce the influence of the errors by using the information from the analyzed images themselves. In this paper we suggest the technique to correct the navigation parameters in such a way. The technique is based on the application of the contour analysis and multiple view geometry methods. These methods make it possible to implement our technique in real time due to the low computational complexity of the contour analysis and multiple view geometry algorithms. The results represented in the paper indicate that the further development and application of the suggested technique for multispectral computer vision systems are promising.

Keywords

Multispectral computer vision system, multiple view geometry, contour analysis, navigation parameters correction, object detection, homography, aircraft.

1 INTRODUCTION

The correct determination of the current aircraft location coordinates and orientation in the space is necessary for the successful execution of the flying missions [Wol01]. Since these parameters registered from the navigation system can contain errors the problem of their correction become urgent. When the aircraft has an on-board multispectral computer vision system such correction can be done using this system. It can be carried out by the comparison of the current image from this system's sensor with the image synthetized for the digital terrain map. In so doing the uncorrected navigation parameters are assumed to be known [GuB08]. The problem can be described mathematically. The main navigation parameters are the aircraft space geographic coordinates λ, φ and h and the Euler's angles γ, θ and ψ which describe the aircraft orientation. The latitude λ and the longitude φ determine the aircraft location in the horizontal plane and h determines its altitude. The roll angle γ, the pitch angle θ and the yaw angle ψ determine the aircraft rotation about its longitudinal axis, its horizontal lateral axis of inertia and the vertical axis respectively. Thus the aircraft location and orientation in the space are completely determined by the six-dimensional vector $\mathbf{v} = (\gamma, \theta, \psi, \lambda, \varphi, h)$. The navigation parameters correction problem reduces finding to the error vector $\Delta\mathbf{v}$. This vector describes the divergence between the true navigation parameters vector $\mathbf{v}_r$ and the vector $\mathbf{v}_s$ with the navigation parameters registered from the navigation system $\Delta\mathbf{v} = \mathbf{v}_r - \mathbf{v}_s$. To solve this problem we assume the vector $\mathbf{v}_s$ is known and the original images from the multispectral computer vision system are available. As the original images from this system we can use, e.g., the image pair in Figure 1. The image in Figure 1a is the terrain aerial photograph registered from the aircraft sensor in the current moment of time. We can see the Moscow River in this image. The image in Figure 1b is the synthetized image generated on the basis of the current navigation parameters vector $\mathbf{v}_s$ and the digital terrain map. In the general case the first Earth

 ISBN 978-80-86943-71-8

surface image can be registered from the sensors which work not only in the visible spectral range but in the other spectral ranges, e.g., infrared range. In the example considered the synthetized image is represented by the lines. These lines describe the main terrain objects' contours. As another alternative the synthetized image can contain the objects' contours filled with the texture. We can notice in Figure 1 that the synthetized image viewpoint differs from the aerial photograph viewpoint. The cause is the existence of the errors when determining the current navigation parameters vector $\mathbf{v}_s$. The discrepancy degree of these images can be seen especially clearly when superimposing the original synthetized image on the aerial photograph. Figure 2 represents two examples of such superimposition. The image in Figure 2b contains the visible horizon and the image in Figure 2a does not. The technique suggested in the paper can be used in both the cases.

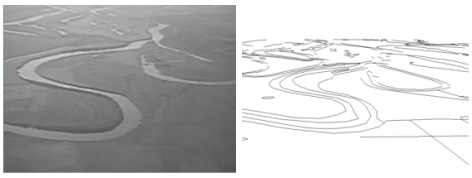

(a) (b)

Figure 1. The original image pair for the analysis: (a) the aerial photograph and (b) the corresponding synthetized image.

(a) (b)

Figure 2. The examples of the simple synthetized image superimposition on the aerial photograph (a) for the images without visible horizon line and (b) for the images with visible horizon line.

The discrepancy occurs because in fact the aerial photograph and the synthetized image are the observed scene projections on different planes. Figure 3 explains the interconnection between them.

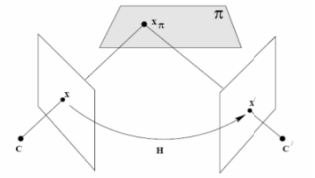

Figure 3. The geometric interconnection between the planes of the original images.

The observed scene is the visible segment of the Earth surface. The desired vector $\mathbf{v}_r$ and the known $\mathbf{v}_s$ specify the positions of the cameras' C and C' centers and the projection planes. So it is required to find the geometric transformation determining the connection between the images. Then it is necessary to find a mathematical method for the calculation of the error vector $\Delta\mathbf{v}$ on the basis of the transformation found.

2 RELATED WORK

The satellite navigation systems (e.g. GPS, GLONASS) in combination with the inertial navigation systems are mainly used in modern aircraft to solve the navigation tasks [GWA01]. The satellite navigation system principle of operation consists in the measurement of the distance from the aircraft antenna to the satellites. When there is no signal from the satellites the autonomous inertial navigation system is used to correct the coordinates. The main point of the inertial navigation is the determination of the object acceleration and its angular velocity with the help of special devices. Then this information is used for the current aircraft location coordinates and the other parameters correction. The navigation parameters calculated this way have the errors. These errors play a significant part in certain tasks, particularly when superimposing the images in the multispectral computer vision systems [FoP01, MVR09, ShS01]. Hence the study of other approaches to construct more precise navigation systems is urgent [BSM04]. Let us assume that the aircraft has a multispectral computer vision system on board. Then the investigation of the possibility to solve the navigation parameters correction problem on the basis of the information from the multispectral computer vision system images analysis is of particular interest [BSM04]. At present, most developed direction in the construction and the improvement of the navigation systems which use the information from the images is devoted to the correlation navigation systems. However, the methods used in such systems are based on the direct comparison of the images' pixels. This requires high computational efforts. At the same time in the multispectral computer vision system the image registered from the aircraft sensor is compared with the image synthetized on the basis of the digital terrain map. Such a synthetized image in fact describes only the main terrain objects' contours. The main idea of using the multispectral computer vision system for the navigation parameters correction is to detect the supporting terrain sections in the available aerial photographs and the synthetized images. These terrain sections are considered as the objects of interest. In the case of the successful detection and comparison of such objects it is possible to perform the navigation parameters correction. To do this the current aircraft location binds to the available terrain map using the found objects. Obviously, such method would work only when the terrain in the images has enough singled out objects. These objects can be

used to compare the aerial photograph and the synthetized image.

The considered problem of the navigation parameters correction using the information from the multispectral computer vision system images and the aircraft navigation system sensors is a complex mathematical problem. We can highlight three main task groups. It is necessary to solve the tasks of each group to derive the navigation parameters correction. These tasks are the detection of the most significant objects in the original images; the comparison of the detected objects with each other on the basis of the found corresponding point pairs on these objects' contours; the finding the geometric transformation which binds the original images, and the navigation parameters correction using the obtained binding information. Next we consider sequentially the known approaches to the solution of the listed tasks. There are a lot of different approaches to object detection and comparison in images. Among them besides the correlation methods we can mark out the image comparison methods based on morphological similarity measures [GoW08] and the methods based on the extraction of the corresponding points using the intensity values in these points' neighborhoods [BET08]. However, we should take into consideration the solvable problem specificity when choosing the methods, viz. we need to work in real time [Lap04], and we have the synthetized image represented by the lines describing the main terrain objects' contours. Therefore it is interesting to investigate more intellectual and less time-consuming methods. The complexity of the object detection in the terrain aerial photograph is also conditioned by the possible distortions of the intensities and geometry of the observed objects. The intensity distortions can be caused by the difference in the registration conditions of the aerial photographs. The influences of the illuminance, the season, the day time, the meteorological conditions, and the sensor quality matter a lot. The geometric distortions are attributed mainly to the difference between the image acquisition viewpoints. This leads to the difference between the forms of the same object in the images for the different viewpoints. In the light of the mentioned circumstances the contour analysis methods application seems the most effective. It does not to take into account the intensity specifics but only the objects' forms [Fur02, NSN13]. The further comparison of the objects on the basis of the comparison of their contours' fragments gives us the possibility to reduce the influence of the geometric distortions and also to solve the problem of the objects partly overlapping. We obtain the vector descriptions of the detected objects using contour analysis methods. Further these descriptions can be used to find corresponding point pairs in the original images. At present the image comparison methods based on the corresponding points are investigated deeply enough for the case when the images have the same nature, e.g. two aerial photographs [BET08]. However, in our case of the images of various natures such methods are inapplicable. It is because these methods are based on the intensity gradient variation analysis but one of the compared images initially consists of lines. Thus it becomes necessary to solve the task of the corresponding point pairs finding in the images on the basis of the contour analysis methods and algorithms. Our tasks are to find the geometric interconnection between two image planes and to determine the camera parameters from the information obtained from these images themselves. Usually to solve these tasks the corresponding point pairs are used. Recently, such approaches have been studied a lot theoretically and practically. The main results are expounded in the multiple view geometry [HaZ04]. This geometry has been rapidly developed in the recent decades. It is known that the affine geometric transformations such as rotation, translation and scaling are implemented within one plane. So we can't use affine transformations to establish the connection between the original images which are the projections to the different planes. Therefore to solve the navigation parameters correction problem using the multispectral computer vision system images it is required to consider the more general class of transformations, viz. the projective geometric transformations [SNN13b].

In this paper we suggest the navigation parameters technique for real time multispectral computer vision systems. This technique is based on the application of the contour analysis [Fur02, NSN13] and multiple view geometry methods [HaZ04].

3 TECHNIQUE AND METHODS OVERVIEW

The methods can be divided into three main groups according to the tasks classification in Section 2.

3.1 Technique Overview

By virtue of the investigations carried out we suggest the following navigation parameters correction technique using the multispectral computer vision system information.

1. The aerial photograph, the synthetized image and the estimated current navigation parameters vector are acquired as the original data.
2. The distinctive objects in the aerial photograph are detected, and the transition to the aerial photograph vector description is performed.
3. The contours' fragments of the objects in the aerial photograph and in the synthetized image are compared.
4. The corresponding point pairs in the available images are found.

5. The corresponding point pairs for the projective geometric transformation calculation are selected.
6. The homography and the cameras' internal calibration matrices are calculated.
7. The Euclidean homography decomposition is done.
8. The navigation parameters determination errors are calculated, viz. the error vector $\Delta\mathbf{v}$.
9. The current aircraft location coordinates are corrected: $\mathbf{v}_r = \mathbf{v}_s + \Delta\mathbf{v}$.

To implement the image object detection and comparison stages it is suggested to use the known algorithms and our specially developed algorithms based on the contour analysis methods application [NSN13, SNN13a]. The application of multiple view geometry methods consists of finding the geometrical interconnection between the planes of the original images and in the algebraic expression of this interconnection [HaZ04, FSS10, SNN13b]. To the effect the information about the corresponding point pairs obtained by the analysis of these images themselves is used. It is known that if the observed scene is a plane (Figure 3) then such interconnection can be described using the homography matrix

$$\mathbf{H} = \begin{pmatrix} h_{11} & h_{12} & h_{13} \\ h_{21} & h_{22} & h_{23} \\ h_{31} & h_{32} & 1 \end{pmatrix}. \qquad (1)$$

However this interconnection between the projection planes of the aerial photograph and the synthetized image is defined implicitly. We can easily recalculate point coordinates of one image to another image plane using the homography matrix $\mathbf{H}$. But to solve the navigation parameters correction problem it is not enough. The projective geometric transformation in the large is defined by all of the homography matrix $\mathbf{H}$ components. However we can highlight the meanings of the particular components of this matrix. The components h_{11}, h_{12}, h_{13}, h_{21}, h_{22}, h_{23} define the scaling, the rotation and the translation. If the remaining components h_{31} and h_{32} are zero then the homography matrix $\mathbf{H}$ defines an affine transformation. Thus the components h_{31} and h_{32} describe directly the projective distortions. The experimental results of the homography matrix $\mathbf{H}$ calculation are considered next. These results show that these components for the analyzed multispectral computer vision system image pairs have the greatest values in magnitude in comparison with the rest of the components. To solve the navigation parameters correction problem it is necessary to estimate the existing errors in their determination in the aircraft navigation system, viz. the error vector $\Delta\mathbf{v}$. After the calculation of the geometric transformation connecting the original images the homography matrix $\mathbf{H}$ is known. The error vector $\Delta\mathbf{v}$ describes the space location differences between the cameras' centers C and C' for the aerial photograph and the synthetized image and between these cameras' orientations. These differences are defined by the translation vector $\mathbf{t}$ and the rotation matrix $\mathbf{R}$ respectively. The translation vector $\mathbf{t}$ is given by $\mathbf{t} = (t_x, t_y, t_z)^T$ and the rotation matrix $\mathbf{R}$ is given by

$$\mathbf{R} = \begin{pmatrix} r_{11} & r_{12} & r_{13} \\ r_{21} & r_{22} & r_{23} \\ r_{31} & r_{32} & r_{33} \end{pmatrix}. \qquad (2)$$

The components of the rotation matrix $\mathbf{R}$ can be determined from the Euler's angles in the following manner:

$$r_{11} = \cos\psi \cdot \cos\theta,\ r_{12} = \cos\psi \cdot \sin\theta \cdot \sin\gamma - \sin\psi \cdot \cos\gamma,$$
$$r_{13} = \cos\psi \cdot \sin\theta \cdot \cos\gamma + \sin\psi \cdot \sin\gamma,$$
$$r_{21} = \sin\psi \cdot \cos\theta,\ r_{22} = \sin\psi \cdot \sin\theta \cdot \sin\gamma + \cos\psi \cdot \cos\gamma,$$
$$r_{23} = \sin\psi \cdot \sin\theta \cdot \cos\gamma - \cos\psi \cdot \sin\gamma,$$
$$r_{31} = -\sin\theta,\ r_{32} = \cos\theta \cdot \sin\gamma,\ r_{33} = \cos\theta \cdot \cos\gamma.$$

Hence if the rotation matrix $\mathbf{R}$ is known it is easy to calculate the Euler's angles (the roll γ, the pitch θ and the yaw ψ): $\gamma = \arctan\dfrac{r_{32}}{r_{33}}$;

$$\theta = \arctan\left(-\frac{r_{31}}{\sqrt{r_{32}^2 + r_{33}^2}}\right);\ \psi = \arctan\frac{r_{21}}{r_{11}}.$$

Thereby the rotation matrix $\mathbf{R}$ makes it possible to calculate the Euler's angle errors $\Delta\gamma$, $\Delta\theta$ and $\Delta\psi$. At the same time we can easily determine the current aircraft location errors $\Delta\lambda$, $\Delta\varphi$, Δh from the known translation vector $\mathbf{t}$. For that it is enough to come from the aircraft coordinate system to the geographical coordinate system. Hence we can completely define the required error vector $\Delta\mathbf{v}$ by the known rotation matrix $\mathbf{R}$ and the translation vector $\mathbf{t}$ and then correct the current aircraft location. So the main problem of the suggested technique implementation is the obtaining the rotation matrix $\mathbf{R}$ and the translation vector $\mathbf{t}$ from the known homography matrix $\mathbf{H}$. This problem is called the Euclidean homography decomposition. At the present time there are a number of approaches to this complex mathematical problem. These approaches underlie the developed algorithms for the Euclidean homography decomposition [MaV07, KBC13]. As a rule to perform such decomposition successfully it is additionally required to know the camera intrinsic calibration matrices $\mathbf{K}$ [IAM04]. If these matrices are unknown nevertheless they can be estimated from the keypoints in the video image sequence obtained from the evaluable cameras [HaZ04].

3.2 Object Detection in the Aerial Photographs and Synthetized Images for the Subsequent Comparison

The synthetized image initially represents the main objects' contour description. These objects are specified in the digital terrain map. But the aerial photograph should be subject to preprocessing for the purpose of the main object detection and obtaining their contours vector description. Only after that the existing objects' contours in both the original images become comparable. The processing and analysis technique of the original aerial photograph consists in the application of a number of algorithms [GoW08]. Since it is required to detect the main objects' contours in the aerial photograph and to represent them in the vector form, the first image processing algorithm which is used is an edge detection algorithm. We can use, e.g., the Canny algorithm or our own gradient algorithm [SNN13a]. Further we can obtain closed contours of the objects existing in the aerial photograph using the morphological processing algorithms. Then it is necessary to discard the insignificant objects and to retain only the main objects, which are probably also exist in the synthetized image. After that we need to obtain the schematic representation of the main objects for the subsequent comparison. So we can smooth over the small insignificant details. To do so, we use the approximating polygon finding algorithm. This algorithm lets us obtain the vector description of the closed contours for the objects of interest with different degrees of detail. This algorithm is based on the approximating polygon vertex selection using local maxima of angle cosine estimations for these vertices. The remaining closed contour points are removed. The angle cosine estimations are calculated using least square fit to a certain number of neighbor points on both the sides of the vertex [SNN13a, NSN13]. After obtaining the vector description for the main objects in original images it is possible to implement the object comparison stage. The objects detected in both the original images are compared with each other. Objects' contours are compared pairwise. A problem is that the same object has in general a different number of vertices in the different contour descriptions. Another problem is that an object can be partly overlapped by something in the image. Because of these problems we estimate the local similarity of the contours. For this purpose an auxiliary subcontour is generated for each vertex of the main analyzed contour $\Gamma = \{(x_1, y_1), (x_2, y_2), \ldots (x_N, y_N)\}$. These subcontours are used for the comparison of the main contour. The examples of the comparing objects' contours marked by the black color with the examples of the generated subcontours marked by the gray color are represented in Figure 4. The axes in Figures 4 and 5 indicate the row and column numbers of the pixels in the sample original images with islands in the Mediterranean Sea.

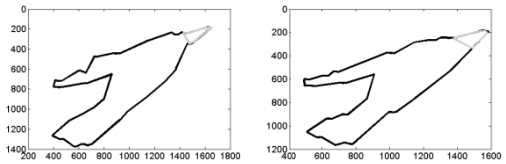

(a) (b)

Figure 4. The examples of the objects' closed contours with the generated subcontours (a) for the first image and (b) for the second image.

3.3 Finding Corresponding Point Pairs on the Detected Objects' Contours

To establish the correspondence between the detected objects' contours fragments we can use different complementary contour analysis algorithms. In particular, we can use the subcontour generation algorithm and then compare these auxiliary subcontours by the autocorrelation function τ. Then each subcontour of one contour is compared to all of the subcontours of the other contour for the purpose of finding the similar fragments of the existing contours. As the similarity measure for subcontours we use the autocorrelation function in combination with additional parameters of the vertex. We calculate the autocorrelation function as follows. The autocorrelation function is a vector τ whose components are $\tau_k = \frac{|(\Gamma_k, \Gamma_0)|}{(\Gamma_0, \Gamma_0)}, \quad k = 1, 2, ..., n-1$

where $(\Gamma_k, \Gamma_0) = \sum_{m=1}^{n} \left((x_m + iy_n) \cdot (x_{k+m(\mathrm{mod}\, n)}) - iy_{k+m(\mathrm{mod}\, n)} \right)$

and $(\Gamma_0, \Gamma_0) = \sum_{m=1}^{n} \left(x_m^2 + y_m^2 \right)$.

The similarity measure for each subcontour γ_m of the second contour and a certain fixed subcontour γ_0 of the first contour is calculated as follows:

$$\Delta_m = \sum_{k=1}^{[n/2]} \left| \tau_k^{(m)} - \tau_k^{(0)} \right|. \qquad (3)$$

The calculated values Δ_m are compared with a given threshold ε. If $\Delta_m < \varepsilon$ the subcontour γ_m is included in the set of the contours close to the subcontour γ_0. Otherwise, it is excluded from this set. The selection among the close subcontours is performed using additional parameters for the comparing main contour vertices such as the vertex angle and the mutual position of the vertex and the other contour vertices. On the basis of this analysis we can select the most likely point pairs belonging to the same fragments of both the contours. To visualize the result the selected corresponding point pairs also can be connected as closed contours. They are represented in such a way as gray contours in Figure 5. This technique involves the step-by-step

implementation of a number of contour analysis algorithms.

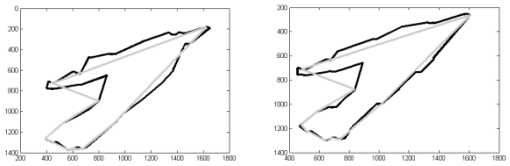

(a) (b)

Figure 5. The automatically found corresponding point pairs on the objects' contours (a) on the contour from the first image and (b) on the contour from the second image.

3.4 Calculation of the Geometric Transformation Connecting the Aerial Photograph and the Synthetized Image

The projective geometric transformation connecting the original images is done using the homography matrix $\mathbf{H}$ which has eight degrees of freedom.

To calculate the matrix $\mathbf{H}$ it is enough to have four correct corresponding point pairs in the original images, viz. the points $R_1(x_1^r, y_1^r)$, $R_2(x_2^r, y_2^r)$, $R_3(x_3^r, y_3^r)$, $R_4(x_4^r, y_4^r)$ in the aerial photograph and the points $S_1(x_1^s, y_1^s)$, $S_2(x_2^s, y_2^s)$, $S_3(x_3^s, y_3^s)$, $S_4(x_4^s, y_4^s)$ in the synthetized image respectively. Besides to determine the homography matrix $\mathbf{H}$ unambiguously it is necessary that no three of these points belonging to one image lie on the same line. Moreover, the experiments show that the most stable results are obtained when the points are as far as possible from each other. To increase the accuracy of the homography matrix $\mathbf{H}$ determination it is desirable to find as many corresponding point pairs as possible. Then we can discard the superfluous point pairs, e.g., by using the RANSAC algorithm [FiB81, BaB02]. We carried out some experiments with this algorithm but we need more investigations to implement it in our technique to determine automatically the required point pairs which can be used directly for the homography matrix $\mathbf{H}$ calculation. The correctness of selecting the desired points is important because the accuracy of this matrix calculation strongly depends on that. Therefore the more corresponding objects are found the more it is likely to find correct point pairs automatically for the homography matrix $\mathbf{H}$ calculation. The correct selection of the corresponding point pairs is a rather difficult image analysis problem. The successful solution of this task is only possible when there is a sufficient quantity of the distinctive objects or their parts in the both the original images. When the four corresponding point pairs are known the homography matrix $\mathbf{H}$ calculation is done as follows. We can shape the matrix using these points' coordinates

$$\mathbf{A} = \begin{pmatrix} x_1^s & y_1^s & 1 & 0 & 0 & 0 & -x_1^s x_1^r & -y_1^s x_1^r \\ x_2^s & y_2^s & 1 & 0 & 0 & 0 & -x_2^s x_2^r & -y_2^s x_2^r \\ x_3^s & y_3^s & 1 & 0 & 0 & 0 & -x_3^s x_3^r & -y_3^s x_3^r \\ x_4^s & y_4^s & 1 & 0 & 0 & 0 & -x_4^s x_4^r & -y_4^s x_4^r \\ 0 & 0 & 0 & x_1^s & y_1^s & 1 & -x_1^s y_1^r & -y_1^s y_1^r \\ 0 & 0 & 0 & x_2^s & y_2^s & 1 & -x_2^s y_2^r & -y_2^s y_2^r \\ 0 & 0 & 0 & x_3^s & y_3^s & 1 & -x_3^s y_3^r & -y_3^s y_3^r \\ 0 & 0 & 0 & x_4^s & y_4^s & 1 & -x_4^s y_4^r & -y_4^s y_4^r \end{pmatrix} \quad (4)$$

and also the vector

$$\mathbf{B} = (x_1^r \quad x_2^r \quad x_3^r \quad x_4^r \quad y_1^r \quad y_2^r \quad y_3^r \quad y_4^r)^T. \quad (5)$$

Then

$$\mathbf{h} = \mathbf{A}^{-1}\mathbf{B} \quad (6)$$

where $\mathbf{h} = (h_{11} \quad h_{21} \quad h_{31} \quad h_{12} \quad h_{22} \quad h_{32} \quad h_{13} \quad h_{23})^T$ is the column vector which elements are the elements of the homography matrix (1).

When the matrix $\mathbf{H}$ is known we can recalculate the coordinates of the synthetized image points $S_i(x_i^s; y_i^s)$ to the aerial photograph plane (the points $R_i(x_i^r; y_i^r)$):

$$\begin{pmatrix} x_i^{r'} \\ y_i^{r'} \\ z_i^{r'} \end{pmatrix} = \mathbf{H}^T \begin{pmatrix} x_i^s \\ y_i^s \\ 1 \end{pmatrix}, \quad \begin{pmatrix} x_i^r \\ y_i^r \end{pmatrix} = \begin{pmatrix} x_i^{r'} / z_i^{r'} \\ y_i^{r'} / z_i^{r'} \end{pmatrix}. \quad (7)$$

After that the transformed synthetized image can be superimposed on the aerial photograph to verify the correctness of the projective geometric transformation. This superimposition result can also be used as the solution of the synthetized image superimposition task with the aerial photograph.

4 RESULTS

In this section the examples of the experimental results are represented. We have developed a number of algorithms to obtain these results [NSN13, SNN13a, SNN13b]. Let us consider the process of the homography matrix $\mathbf{H}$ calculation and the implementation of the corresponding synthetized image transformation to the aerial photograph plane for the original images in Figure 1. When analyzing such images it should be taken into consideration that the most distinctive objects which can be detected in the Earth surface images are water objects, viz. the rivers, the lakes, the seashores, the islands in the sea. That is why when there are such objects in the images the task of finding corresponding point pairs is significantly simplified. When there are no distinctive objects in the images the suggested technique can't be implemented. The water object is the Moscow River for both the examples represented in Figure 2. To carry out the experiment the following four corresponding point pairs belonging to the river contours in the aerial photograph and in

 ISBN 978-80-86943-71-8

the synthetized image are selected (Figure 6): $R_1(42;200)$ and $S_1(118;274)$, $R_2(412;358)$ and $S_2(401;378)$, $R_3(409;152)$ and $S_3(391;241)$, $R_4(321;77)$ and $S_4(321;187)$. The homography matrix $\mathbf{H}$ is calculated by the selected point pairs in accordance with formulas (4-6):

$$\mathbf{H} = \begin{pmatrix} 1{,}1783 & -0{,}0150 & -0{,}0001 \\ -0{,}1999 & 1{,}2316 & -0{,}0003 \\ -46{,}2831 & -154{,}8272 & 1{,}0000 \end{pmatrix}. \quad (8)$$

Further we can perform the projective geometric transformation of the original synthetized image to the aerial photograph plane by formulas (7). The obtained transformed synthetized image is represented in Figure 7.

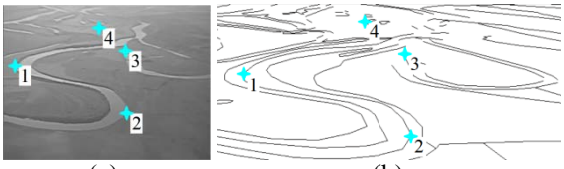

(a) (b)

Figure 6. The corresponding point pairs for the homography matrix calculation (a) in the aerial photograph and (b) in the synthetized image.

Figure 7. The synthetized image after the projective geometric transformation.

We can compare the original synthetized image in Figure 1b and the synthetized image after the projective geometric transformation in Figure 7. We can notice that both of them represent the models of the same terrain for the different viewpoints. To verify that the new viewpoint corresponds to the original aerial photograph in Figure 1a the transformed synthetized image can be imposed on the original aerial photograph. The result of such superimposition is shown in Figure 8a. The effectiveness of the aerial photograph and the synthetized image superimposition using the geometric transformation based on the homography matrix follows from the set of successful experiments carried out by the described technique. The result of the analogous experiment carried out for the example in Figure 2b is represented in Figure 8b. In this case the following homography matrix $\mathbf{H}$ describing the geometric interconnection between the original images is calculated by the four selected point pairs:

$$\mathbf{H} = \begin{pmatrix} 1{,}7375 & -0{,}12 & -0{,}0004 \\ -1{,}0284 & 2{,}1215 & 0{,}0013 \\ 133{,}4345 & -196{,}3565 & 1{,}0000 \end{pmatrix}. \quad (9)$$

(a) (b)

Figure 8. The superimposition of the synthetized image geometrically transformed with the original aerial photograph (a) for the first example and (b) for the second example.

5 CONCLUSION AND FUTURE WORK

In this paper the navigation parameters correction technique based on the multispectral computer vision system images is suggested. The application of the contour analysis and the multiple view geometry methods makes it possible to perform such correction in real time. The obtained theoretical and practical results argue that the research continuation in the considered direction is promising. The first six stages of the suggested technique are already implemented. But it is necessary to optimize the developed algorithms. The remaining stages require deeper mathematical study and then implementation. As an allied task we can indicate the image superimposition problem in the multispectral computer vision system [SNN13a]. The solution of this task follows logically from the solution of the navigation parameters correction problem. Moreover, the successful application of the suggested navigation parameters correction technique on the basis of the multiple view geometry methods will make it possible to significantly reduce or to completely eliminate the need to exhaustively search for the correct viewpoint for the synthetized image. But this is only possible when there are enough distinctive objects which can be detected in the images. The continuation of this research work will provide the possibility to use the multispectral computer vision system for aircraft navigation parameters correction. As the main directions of this continuation work we suggest the following: the improvement of the contour analysis algorithms for automatically finding the corresponding point pairs on the objects' contours; the development of the algorithms for verifying the correctness of the projective geometric transformation calculation on the basis of estimating the quality of the objects' contours superimposition; the implementation of the algorithms for the camera intrinsic calibration matrix determination by the images from this camera; the investigation of the Euclidean homography decomposition methods and algorithms; and the experimental validation of all the algorithms which are additionally developed to implement the navigation parameters correction technique using the multispectral computer vision system.

6 REFERENCES

[BaB02] Pierre A. J. Bayerl, Gregory Baratoff, An Interactive Vision-Based Tool for Model-Based Scene Calibration of Augmented Reality Environments, in Proceedings of 10th International Conference on Computer Graphics, Visualization and Computer Vision (WSCG'2002), Plzen, Czech Republic, 2002, pp. 55-62.

[BET08] Herbert Bay, Andreas Ess, Tinne Tuytelaars, and Luc Van Gool, Speeded-Up Robust Features (SURF), Elsevier, CH-8092 Zurich, B-3001 Leuven, 2008, 14 p.

[BSM04] Fadi Atef Bayoud, Jan Skaloud, Bertrand Merminod, Photogrammetry-derived Navigation Parameters for INS Kalman Filter Updates, Proceedings of the XXth International Society of Photogrammetry and Remote Sensing (ISPRS) Congress, Istanbul, Turkey, 2004, pp. 252-257.

[FiB81] Martin A. Fischler and Robert C. Bolles, Random Sample Consensus: A Paradigm for Model Fitting with Applications to Image Analysis and Automated Cartography, Communications of the Association for Computing Machinery (ACM), 1981, vol. 24, no. 6.

[FoP01] David A. Forsyth and Jean Ponce, Computers Vision: A Modern Approach, New York, Prentice-Hall, 2001, 792 p.

[FSS10] Shinji Fujiyama, Fumihiko Sakaue, Jun Sato, Multiple View Geometries for Mirrors and Cameras, In Proc. IEEE Conference on Computer Vision and Pattern Recognition (CVPR), San Francisco, CA, USA, 2010, pp. 45-48.

[Fur02] Yakov A. Furman (ed.), Contour Analysis Introduction and its Image and Signal Processing Application, Moscow, Nauka, 2002, 592 p.

[GoW08] Rafael C. Gonzales and Richard E. Woods, Digital Image Processing, 3nd ed. New York, Prentice-Hall, 2008, 954 p.

[GuB08] Vishisht Gupta, Sean Brennan, Terrain-based vehicle orientation estimation combining vision and inertial measurements, Journal of Field Robotics (JFR), vol. 25, no. 3, 2008, pp. 181-202.

[GWA01] Mohinder S. Grewal, Lawrence R. Weill, Angus P. Andrews, Global Positioning Systems, Inertial Navigation, and Integration. John Wiley & Sons, Inc., 2001, 408 p.

[HaZ04] Richard I. Hartley and Andrew Zisserman, Multiple view geometry in computer vision, Cambridge University Press, 2nd edition, 2003, 673 p.

[IAM04] Ivo Ihrke, Lucas Ahrenberg, and Marcus Magnor, External camera calibration for synchronized multi-video systems, in Proceedings of 12th International Conference on Computer Graphics, Visualization and Computer Vision (WSCG'2004), Plzen, Czech Republic, 2004, pp. 537–544.

[KBC13] Bernd Krolla, Gabriele Bleser, Yan Cui, Didier Stricker, Representing Feature Location Uncertainties in Spherical Images, in Proceedings of 21th International Conference on Computer Graphics, Visualization and Computer Vision (WSCG'2013), Plzen, Czech Republic, 2013, pp. 187-194.

[Lap04] Phillip A. Laplante Real-Time Systems Design and Analysis. New York: John Wiley & Sons, 2004, 480 p.

[MaV07] Ezio Malis and Manuel Vargas Deeper, Understanding of the Homography Decomposition for Vision-Based Control.Rocquencourt: INRIA/RR-6303, 2007, 90 p.

[MVR09] Amit Mukherjee, Miguel Velez-Reyes, Badrinath Roysam, Interest Points for Hyperspectral Image Data, IEEE Transactions on Geoscience and Remote Sensing (TGARS), vol. 47, no. 3, 2009, pp. 748-760.

[NSN13] Anatoly I. Novikov, Victoria A. Sablina, Michael B. Nikiforov, Alexander A. Loginov, Contour Analysis and Image Superimposition Task in Computer Vision Systems, The 11th International Conference «Pattern Recognition and Image Analysis: New Information Technologies» (PRIA-11-2013), Samara, Russian Federation, 2013, vol. I, pp. 282-285.

[ShS01] Linda G. Shapiro and George C. Stockman, Computer Vision. New York, Prentice-Hall, 2001, 608 p.

[SNN13a] Victoria A. Sablina, Anatoly I. Novikov, Michael B. Nikiforov, and Alexander A. Loginov, An Approach to the Image Superimposition Problem in Multispectral Computer Vision Systems,2nd Mediterranean Conference on Embedded Computing (MECO), Budva, Montenegro, 2013, pp.117-120.

[SNN13b] Victoria A. Sablina, Anatoly I. Novikov, Michael B. Nikiforov, Geometric Transformations for the Map Image Superimposition with the Aerial Photograph, Proceedings of the VIIIth International Scientific and Information Technologies (CSIT), Lviv, Ukraine, 2013, pp. 31-33.

[Wol01] James Wolper, Understanding Mathematics for Aircraft Navigation, McGraw Hill Professional, 2001, 260 p.